Available online at www.sciencedirect.com
SCIENCE DIRECT®
Journal of Nuclear Materials 352 (2006) 42–49
journal of nuclear materials
www.elsevier.com/locate/jnucmat

Resistivity recovery simulations of electron-irradiated iron: Kinetic Monte Carlo versus cluster dynamics

J. Dalla Torre, Chu-Chun Fu *, F. Willaime, A. Barbu, J.-L. Bocquet

Service de Recherches de Métallurgie Physique, CEA/Saclay, 91191 Gif-sur-Yvette, France

Abstract

The isochronal resistivity recovery in high purity α-iron irradiated by electrons was successfully reproduced by a multiscale modelling approach. The stability and mobility of small self-defect clusters determined by ab initio methods were used as input data for an event based Kinetic Monte Carlo (KMC) model, used to explore the defect population evolution during the annealing and to extract the resistivity recovery peaks. In this paper, we investigate the possibility of using an efficient mesoscale model, the Cluster Dynamics (CD), instead of KMC in this approach. The comparison between the two methods for various CD initial conditions shows the importance of spatial correlations between defects, which are neglected in the CD model. However, using appropriate initial conditions, e.g. starting from the concentration of Frenkel pairs after the uncorrelated stage I_E, the CD model captures the main characteristics of subsequent defect population evolution, and it can therefore be used for fast and semi-quantitative investigations.

PACS: 61.72.Ji; 61.72.Bb; 61.80.−x

1. Introduction

The behavior of materials under irradiation is a typical multiscale phenomenon since the microstructural evolution over hours or years results from atomic-scale defects evolving at the picosecond scale. The predictive simulations of such phenomena in metals in general, and in iron in particular, rely on various models covering these different time and length scales:

(i) First principles calculations provide accurate information concerning point defect energetics and migration mechanisms [1–3]. They are computationally very demanding and are therefore usually limited to structure optimizations using supercells of a few hundreds of atoms.
(ii) Empirical-potential molecular-dynamics is widely used to investigate properties of defects on the nanosecond scale, their formation during irradiation [4], their migration [5,6] and their clustering [7]. However, the validity of such an approach is restricted to the validity of the interatomic potential used.
(iii) Kinetic Monte Carlo (KMC) simulations are capable of simulating long time (hours and beyond) behavior of material microstructure evolution [8,9]. However the validity of kinetic

* Corresponding author.

0022-3115/$ - see front matter © 2006 Elsevier B.V. All rights reserved.
doi:10.1016/j.jnucmat.2006.02.040

Monte Carlo simulations are restricted to the validity of defect properties included in the input database: primary irradiation damage, migration and stability of defects.

(iv) Cluster Dynamics (CD) models based on rate theory are widely used to simulate the behavior of materials under irradiation over even longer times. The CD method requires small computational resources and therefore its ability to explore time scales on the order of a reactor lifetime constitutes one of its most important advantage. In addition to the limitation regarding the input data, which is the same as for KMC, the CD method suffers from another drawback coming from the basic hypothesis of uniform spatial distribution of defects: it can not deal with spatial correlations between defects.

On the experimental side, detailed information on defect properties can be extracted from resistivity recovery experiments. The principle of the experiment is to irradiate materials at low temperature and to raise the temperature gradually in order to thermally activate a sequence of mechanisms of defect migration, dissociation or reaction. In the experiments by Takaki et al. [10], high purity iron – with a carbon content lower than 1 atomic part per million – is irradiated by electrons at low temperature (4.5 K). A sequence of abrupt sample resistivity changes (recovery stages) are observed during isochronal annealing. The plots of the derivative of the resistivity recovery (DRR) as function of temperature show peaks associated to the different stages. According to the experiments and interpretations of Takaki et al. [10] the different stages are identified as follows:

- Close-pair stages are observed at 23, 39, 51, 67, 89 and 101 K. They are associated to the recombination of self-interstitial atoms, I, and vacancies, V, forming bound pairs.
- The stage observed at 107.5 K, named I_{D2} for historical reasons, is connected to the recombination of correlated pairs of defects: freely migrating self-interstitial atoms recombine with their own respective vacancies.
- Stage I_E (in the range 123–144 K for the doses considered) is the uncorrelated recovery stage: freely migrating self-interstitial atoms now escape from their original vacancies and recombine with vacancies from other Frenkel pairs.
- Stage II (164–185 K) is proposed to result from the migration of di-interstitials, I_2.
- Stage III (220–278 K) is suggested to result from V migration.
- Stage IV, the extra stage observed only at high doses between 520 and 550 K, is attributed to the break-up of clusters formed near stage III.

In a previous article [1], we proposed a multiscale simulation of these experiments that succeeded in reconciling the theoretical approach with experimental evidences presented by Takaki et al. [10]. First, detailed ab initio calculations were performed to determine the energetics and migration properties of defects induced by electron irradiation; next, these results were used as input data for an event based KMC model [11,12]. The evolution of the defect population as a function of temperature increase was simulated up to 700 K. Resistivity recovery and then DRR were calculated and compared with the experimental data. In the present paper, we focus on the ability of CD-type models – which are faster but more approximate – to replace KMC for the kinetic step of the multiscale simulation of this particular experiment, using the same ab initio data as inputs.

The damage accumulation under irradiation is a critical test for the CD method [13]. The irradiation damage induces important spatial correlations in particular for neutron irradiation since defects are created in displacement cascades. Even under electron irradiation, the positions of the self-interstitial atom and of the vacancy are still correlated in the creation of a Frenkel pair. A comparison between different KMC models and the CD approach was performed in the case of the irradiation of a thin plate by electrons considering that I and V are created homogeneously in the volume (spatial correlations between defects are thus avoided) [9]. An overall agreement was obtained, with a better agreement for the slowest defects. Here we investigate how the CD method performs in a more realistic case, with an initial damage with moderate spatial correlation between defects, but where a rather high accuracy is needed for the comparison with experiments.

2. Simulation methods

2.1. Ab initio defect energetics

The ab initio calculations were performed in the framework of the Density Functional Theory within

the Generalized Gradient Approximation (GGA) with spin polarization using the SIESTA code (Spanish Initiative for Electronic Simulations with Thousands of Atoms) [14]. Core electrons were replaced by nonlocal norm-conserving pseudopotentials, and 10 numerical pseudo atomic orbitals per atom were used to represent valence electrons. This allows to reach an accuracy similar to that of conventional plane wave methods but with less computational cost. All calculation details were the same as in Ref. [1]. The calculations were performed at zero pressure in the body centered cubic structure of ferromagnetic α-Fe using supercells of 128 atomic sites and a $3 \times 3 \times 3$ shifted k-point grid.

The results obtained for vacancy and interstitial-type clusters are summarized in Fig. 1. Vacancy-type clusters tend to form compact structures, with the peculiar point that di-vacancies are second-neighbors. Their migration proceeds by successive nearest-neighbor jumps of the mono-vacancies. In contrast with previous empirical potential calculations, V_3 and V_4 are found to have migration energies significantly lower than that of V and V_2. Interstitial-type clusters up to I_4 are found to be made of parallel $\langle 1\,1\,0 \rangle$ dumbbells. I, I_2 and I_3 migrate by simultaneous or successive nearest-neighbor jumps of the dumbbells, via the Johnson mechanism [2].

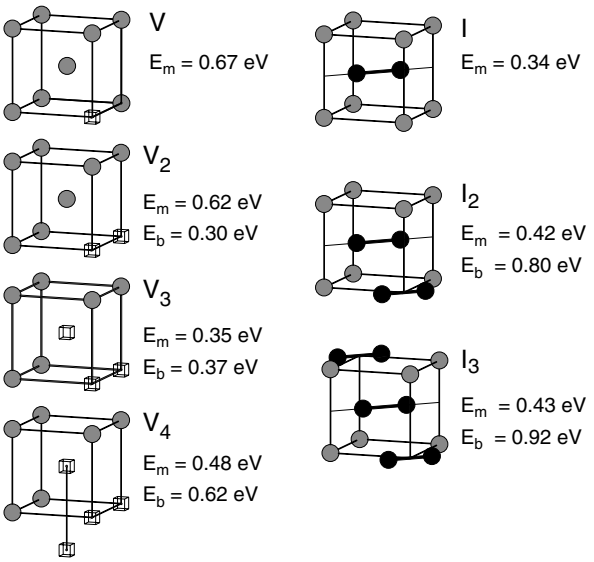

Fig. 1. Properties of small vacancy and interstitial clusters in iron, as obtained from ab initio calculations. For each defect, the lowest energy configuration is schematically represented, and the calculated migration and binding energies are indicated.

2.2. Event-based Kinetic Monte Carlo

We have used an event-based KMC model [11] as implemented in the JERK code [12]. In this model the different defects are considered as objects i.e. the detailed atomic configuration is not treated. The objects are characterized by their continuous space coordinate, their nature (here we consider point defects, I and V, and defect clusters made of n self-interstitial atoms or vacancies, I_n and V_n), shape (spherical here), mobility and dissociation rates. When mobile a defect can diffuse to interact with another one either to form a cluster or to annihilate on an anti-defect. These processes are the result of elementary diffusion jumps (e.g. exchange mechanism for a vacancy to a nearest neighbor lattice site). Instead of considering these elementary jumps, the jumps of mobile objects are bunched into trajectories and the migration and reaction of objects constitute an event that is proceeded in a single Monte Carlo step. This is the major difference between the present and other KMC models, namely atomistic [15] and object [8] ones. One defect may interact with all other defects in the simulation cell and the defects in the image cells resulting from periodic boundary conditions. The reaction between defects in such a medium is a many body question that is approximated in JERK through the superposition of binary interactions of defects in the simulation cell and through an average interaction method using concentric shells of image defects as detailed in Ref. [12].

The JERK method was shown to reproduce defect concentrations with an accuracy of less than 5% in test cases where analytical or numerical solutions could be obtained [12].

2.3. Cluster dynamics

The CD technique describes the time evolution of the cluster size distribution through time and length scales in the macroscopic range [16]. The concentrations of clusters C_n (number of clusters per site) containing n defects obey the differential equations [17]:

$$\frac{\mathrm{d}C_n}{\mathrm{d}t} = G_n + \sum_m w_{m\to n} C_m - \sum_m w_{n\to m} C_n, \qquad (1)$$

where G_n is the production rate of clusters of size n by the irradiating particles, $w_{m\to n}$ is the transition rate per unit concentration from the cluster of size m to the cluster of size n.

The irradiation produces defects and anti-defects (overlined in the following) i.e. self-interstitial atoms and vacancies in equal numbers. The second term of the right hand side of Eq. (1) can be divided into three contributions: (i) larger clusters can emit clusters of size k restricted here to $k = 1$, which is the dominant reaction, (ii) smaller clusters can capture defects, (iii) larger clusters can capture anti-defects:

$$\sum_m w_{m\to n} C_m = \alpha_{n+1,n} C_{n+1} + \sum_k \beta_{n-k,k} C_k C_{n-k} + \sum_k \beta_{n+k,\bar{k}} C_{\bar{k}} C_{n+k}, \quad (2)$$

and similarly, we can write:

$$\sum_m w_{n\to m} C_n = \alpha_{n,n-1} C_n + \sum_k (1+\delta_{nk}) \beta_{n,k} C_k C_n + \sum_k \beta_{n,\bar{k}} C_{\bar{k}} C_n, \quad (3)$$

where $\alpha_{n+1,n}$ is the rate of emission of a single defect from a cluster of size $n+1$, and $\beta_{n,k}C_k$ is the agglomeration rate of clusters of size k on a cluster of size n.

The agglomeration coefficient of clusters is given by [18]:

$$\beta_{n,k} = 4\pi r_{nk} \frac{[(1-\delta_{nk})D_n + D_k]}{\Omega} \quad (4)$$

where D_n is the diffusion coefficient of a cluster of size n, r_{nk} the capture radius given in [12], and Ω the atomic volume.

The dissociation rates are deduced from the equilibrium condition of zero flux:

$$\alpha_{n+k,k} = 4\pi r_{nk} \frac{[(1-\delta_{nk})D_n + D_k]}{\Omega} \exp[E^b_{n,k}/k_B T] \quad (5)$$

where $E^b_{n,k}$ is the binding energy of a cluster of size n and a cluster of size k, k_B is the Boltzmann constant and T the temperature.

2.4. Kinetic Monte Carlo and Cluster Dynamics setup

The input parameters for the KMC and CD calculations are essentially the same: diffusion coefficients, reaction distances and binding energies of point defects to clusters. In a dissociation event, we have chosen to attribute random positions for the emitted defects [12] in the KMC simulation, this choice being consistent with the hypothesis of uniform concentration averaging in the CD method. The concentrations of defects produced by the irradiation are obtained from the experimental values of the resistivity of the sample and that of a Frenkel pair [19]. The experimental results are in the dose range of $\sim 2\times10^{-6}$–200×10^{-6} displacement per atom (dpa). The JERK simulations start at 77.2 K, after the close pair recombination stages and far before the correlated pair recombination stage I_{D2} which results from the free migration of self-interstitial atoms. The remaining Frenkel pair concentration before stage I_{D2} is estimated from experiments to be 60% of the initial damage [10]. In the CD simulations we start with various initial conditions. (i) Only Frenkel pairs (noted FP) are created and the simulations start at 77.2 K. The initial conditions are identical to the KMC simulations except that I–V spatial correlations are not accounted for in the CD simulations. (ii) Only Frenkel pairs are created but the simulation starts after stage I_E. The concentration of Frenkel pairs is obtained from the total damage remaining after stage I_E in the KMC. (iii) The detailed concentrations of I, V, I_n and V_n are extracted from the KMC simulations after stage I_E and serve as input for the CD simulation. More simulation setup details are described in Ref. [1].

2.5. Kinetic Monte Carlo results

It was shown that starting from these ab initio defect properties, the JERK KMC method successfully reproduces the resistivity recovery experiment of Takaki et al. in pure iron [1]. The different peak positions I_{D2}, I_E, II, and III as well as the dose effects (shifts of peaks as dose increases) are indeed quantitatively reproduced. The discrepancies between experimental and simulated peak positions are compatible with the accuracy expected for the ab initio input energies, in view of the approximations in the pseudopotential and exchange correlation functional (GGA). For instance the discrepancy observed for stage III corresponds to an error of 0.1 eV on migration energies of vacancy-type defects.

From the simulated evolution of the defect population it can be concluded that stages I_{D2} and I_E are the results of the three dimensional migration of self-interstitial atoms, and that stage II is produced by the migration of I_2 and I_3. More surprisingly, V but also small V_n clusters contribute to stage III. This result supports the interpretation of vacancy-type defect migration in stage III. At high dose, immobile V_n form during stage III and dissociate during stage IV.

3. Results

The CD simulation results with the three different initial conditions are now compared with the reference KMC results described above, as shown in Fig. 2(a) and (b) which correspond to low and high dose respectively. For initial conditions (i), we find in the CD simulation that stages I_{D2} and I_E fuse into a single stage, as expected from the fact that the splitting into two distinct stages is the direct consequence of the spatial correlation between the I and V. The intensity of the CD first peak is much smaller than the I_{D2} peak of the reference KMC simulations indicating that a small fraction of Frenkel pairs recombines in the CD simulations, with direct consequences on the following stages. The intensity of stages II, III and IV in the CD simulations are indeed about 10 times more intense than in the KMC simulations. The defects that have not recombine in the CD first stage namely contribute in the subsequent stages. The positions of stages II and III are shifted to lower temperatures. This is a dose-like effect and the apparent improved agreement with experiments results from a cancellation of errors.

For initial conditions (ii), the peak intensities resulting from CD are too low by a factor of two, and the peak positions of stages II and III are shifted toward higher temperature when compared with the KMC. The initial concentration of defects in the CD does not represent properly the defect concentration in the KMC: all the interstitial type defects are single self-interstitial atoms in the CD simulations, while after stage I_E they are all in clusters according to KMC simulations. As a consequence a large fraction of I recombines with V at the very beginning of the CD simulations and the subsequent defect population is underestimated.

It appears that initial conditions (iii) are the only ones which are appropriate to accurately reproduce

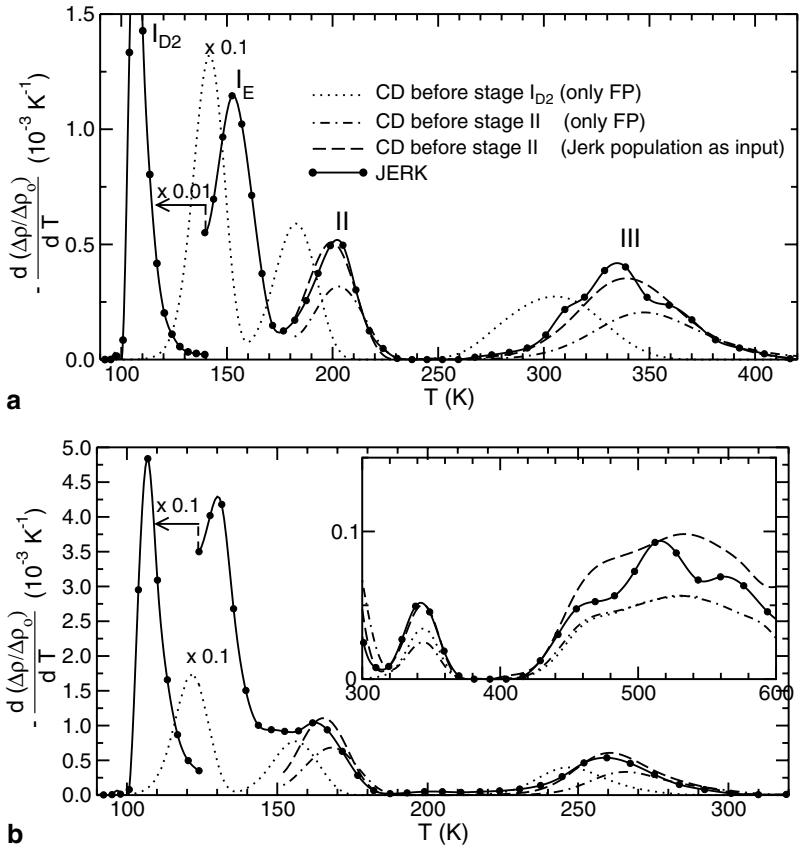

Fig. 2. Isochronal resistivity recovery in iron after irradiation by 3 MeV electrons at (a) low (2×10^{-6} dpa) and (b) high (200×10^{-6} dpa) doses. The CD results are reported with initial conditions (i), (ii), and (iii) as detailed in the text. They are compared with the reference KMC results. $\Delta\rho_0$ and $\Delta\rho(T)$ are the radiation induced resistivity at 4.2 K and temperature T respectively.

the kinetics of the defect annealing. In Fig. 2(a) and (b) the agreement turns out to be excellent, the intensity and peak positions are very satisfactory. In Fig. 3, we examine in more detail the population of interstitial- and vacancy- type defects as predicted by the KMC and the CD simulations after stages II (204 K) and III (309 K) in the high dose simulation. The populations match well for both interstitial- and vacancy-type defects. The vacancy-type defects present a gap between V_2 and V_5 because of the high mobility of V_3 and V_4.

Note that there is a small discrepancy between CD and KMC in the high dose simulations: the intensity near 150 K in the KMC is higher than in the CD. The KMC simulations indicate a sustained recombination of defects between stage I_E and II that may reveal some remaining of spatial correlations between defects.

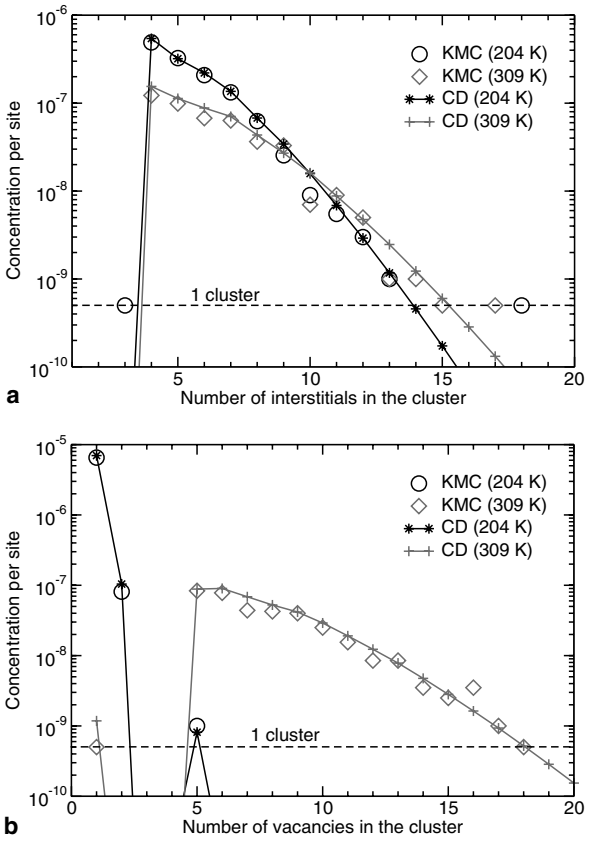

Fig. 3. Size distributions of (a) interstitial-type and (b) vacancy-type clusters after stage II (204 K) and stage III (309 K), as given by KMC and CD simulations at the highest dose. The dashed horizontal line (noted 1 cluster) indicates the concentration corresponding to a single cluster in the simulation cell.

In order to evidence spatial correlations, we have calculated the radial distribution function $G(r)$ between defects – without discriminating between vacancy- and interstitial-type defects for simplicity – in the highest irradiation dose. $G(r)$ is the ratio between the average density at a distance r from any given defect and the equivalent density in an ideal gas with the same average density. It is computed from defects contained into spherical shells of thickness $1a$, where a is the lattice parameter of iron. This definition implies that $G(r) = 1$ corresponds to an homogenous distribution of defects such as in the CD case while deviations from 1 are associated to spatial correlations. Below the recombination distance, we expect $G(r) = 0$. The results for temperatures corresponding to the maximum of the stages I_{D2}, I_E, II, and III respectively are plotted in Fig. 4.

At stage I_{D2}, $G(r)$ shows a single peak with a maximum near $4a$, which is the initial distance between a vacancy and an interstitial within a Frenkel pair in the simulation. This peak remains during the annealing until stage III is reached. During I_{D2} only I–V pairs contribute to the $G(r)$ peak. At higher temperatures we find two contributions to the peak. The first one results from the fact that I-type defects are at about $4a$ from the vacancy-type defects as expected from the initial damage. The second contribution comes from correlations between pairs of V-type defects. The latter can be explained through three body correlations of one I-type defect with two V-type defects as follows. During the initial dose accumulation, some Frenkel pairs are

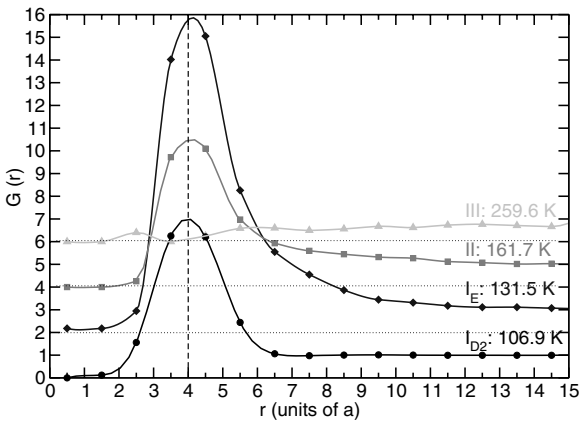

Fig. 4. Radial distribution functions, $G(r)$, between defect-clusters at different stages of the high dose resistivity recovery. The distances are expressed in units of the lattice parameter of bcc iron, $a = 2.87$ Å.

initially so close from each other that I_2–V–V arrangements form spontaneously since the reaction distance between I is larger than that between V. The same three body I_2–V–V arrangements can also be obtained when I migration is activated: when one of the self-interstitial atom of a set of two Frenkel pairs migrates it can indeed either annihilate on one of the vacancies or form a di-interstitial with the other self-interstitial atom. These I_2–V–V arrangements are frozen until the migration of one of the three defects is activated. At increasing temperature, the average density of defects decreases but these arrangements remain and strongly contribute to the $G(r)$. At stage II, I_2 and I_3 begin to migrate and the $G(r)$ peak intensity decreases, but e.g. I_4–V–V can also be formed due to reactions between migrating I-type defects, contributing to an increase in the $G(r)$ intensity. The correlation is completely lost at stage III, when vacancies become mobile (Fig. 4). Small V-type clusters are formed in this stage, but they do not preserve the spatial correlations due to their high mobility.

4. Conclusions

We have investigated the ability of cluster dynamics methods based on rate equation theory to replace the KMC method for the multiscale simulation of resistivity recovery experiments in high purity iron, starting from an ab initio data base of defect properties. We found that:

1. The CD simulation yields only one stage associated with interstitial migration, instead of two (I_{D2} and I_E). The splitting into two peaks is indeed the consequence of the initial spatial correlation between the I and V in a created Frenkel pair.
2. A quantitative agreement for the remaining peaks is obtained only when the CD simulations start after stage I_E and when the exact population of defects (I, I_n, V and V_n) after stage I_E determined from the kinetic Monte Carlo simulations are used as input data. A cluster dynamics simulation therefore requires a preliminary KMC simulation to obtain a realistic distribution of defect population after the two first stages but this part of the simulation is the most computationally demanding one with JERK. However, using intermediate initial conditions, namely starting from the concentration of Frenkel pairs after stage I_E, cluster dynamics captures the main characteristics of stages II and III, and it can therefore be used for fast and semi-quantitative studies.
3. Spatial correlations under high dose electron irradiation are evidenced by the KMC simulations. I–V correlations dominate in the initial stage (I_{D2}), but unexpected three body defect arrangements (I_n–V–V) formed in early stages are found to cause V–V correlations that become important above stage I_{D2} and remain until stage III.

This comparison evidences that after electron irradiation in iron subtle spatial correlations between defects remain far after the recombination of correlated pairs, in particular at high doses. However the cluster dynamics method is expected to capture the main characteristics of defect population evolution, after correction for the recombination of correlated interstitial–vacancy pairs.

Acknowledgements

This work was supported by the PERFECT European Integrated Project under Contract No. FI6O-CT-2003-508840 and by the joint research program SMIRN between EDF, CEA and CNRS.

References

[1] C.C. Fu, J. Dalla Torre, F. Willaime, J.L. Bocquet, A. Barbu, Nat. Mater. 4 (2005) 68.
[2] C.C. Fu, F. Willaime, P. Ordejón, Phys. Rev. Lett. 92 (2004) 175503.
[3] C. Domain, C.S. Becquart, Phys. Rev. B 65 (2001) 024103.
[4] D.J. Bacon, F. Gao, Y.N. Osetsky, J. Nucl. Mater. 276 (2000) 1.
[5] N. Soneda, T. Diaz de la Rubia, Phil. Mag. A 81 (2001) 331.
[6] J. Marian, B.D. Wirth, A. Caro, B. Sadigh, G.R. Odette, J.M. Perlado, T. Diaz de la Rubia, Phys. Rev. B 65 (2002) 144102.
[7] N. Soneda, T. Diaz de la Rubia, Phil. Mag. A 78 (1998) 995.
[8] M.J. Caturla, N. Soneda, E. Alonso, B.D. Wirth, T. Diaz de la Rubia, J.M. Perlado, J. Nucl. Mater. 276 (2000) 13.
[9] A. Barbu, C.S. Becquart, J.-L. Bocquet, J. Dalla Torre, C. Domain, Phil. Mag. 85 (2005) 541.
[10] S. Takaki, J. Fuss, H. Kugler, U. Dedek, H. Schultz, Rad. Eff. 79 (1983) 87.
[11] J.M. Lanore, Rad. Eff. 22 (1974) 153.
[12] J. Dalla Torre, J.-L. Bocquet, N.V. Doan, E. Adam, A. Barbu, Phil. Mag. 85 (2005) 549.
[13] A.V. Barashev, D.J. Bacon, S.I. Golubov, J. Nucl. Mater. 276 (2000) 243.
[14] J.M. Soler, E. Artacho, J.D. Gale, A. Garcia, J. Junquera, P. Ordejón, D. Sanchez-Portal, J. Phys. Cond. Matter 14 (2002) 2745.
[15] F. Soisson, G. Martin, Phys. Rev. B 62 (2000) 203.

[16] A.H. Duparc, C. Moingeon, N. Smetniansky-de-Grande, A. Barbu, J. Nucl. Mater. 302 (2002) 143.
[17] L.K. Mansur, J. Nucl. Mater. 216 (1994) 97.
[18] T.R. Waite, Phys. Rev. 107 (1957) 463.
[19] F. Maury, M. Biget, P. Vajda, A. Lucasson, Phys. Rev. B 14 (1976) 5303.